Bioactive Materials xxx (xxxx) xxx

Contents lists available at ScienceDirect

Bioactive Materials

journal homepage: www.keaipublishing.com/en/journals/bioactive-materials

Adhesive anastomosis for organ transplantation

Kang Liu [a,1], Hang Yang [b,c,1], Gaobo Huang [a,1], Aihua Shi [a], Qiang Lu [a], Shanpei Wang [a], Wei Qiao [d], Haohua Wang [a], Mengyun Ke [a], Hongfan Ding [a], Tao Li [a], Yanchao Zhang [a], Jiawei Yu [a], Bingyi Ren [a], Rongfeng Wang [a], Kailing Wang [a], Hui Feng [a], Zhigang Suo [c,***], Jingda Tang [b,**], Yi Lv [a,*]

[a] National Local Joint Engineering Research Center for Precision Surgery and Regenerative Medicine, Department of Hepatobiliary Surgery, First Affiliated Hospital of Xi'an Jiaotong University, Xi'an, 710061, Shaanxi Province, China
[b] State Key Lab for Strength and Vibration of Mechanical Structures, International Center for Applied Mechanics, Department of Engineering Mechanics, Xi'an Jiaotong University, Xi'an, 710049, China
[c] John A. Paulson School of Engineering and Applied Science, Kavli Institute for Bionano Science and Technology, Harvard University, Cambridge, MA, 02138, USA
[d] Hepatobiliary Surgery Department, Shaanxi Provincial People's Hospital, Xi'an, 710068, Shaanxi Province, China

ARTICLE INFO

Keywords:
Magnet
Hydrogel
Adhesive
Anastomosis
Liver transplantation

ABSTRACT

The recent development of tough tissue adhesives has stimulated intense interests among material scientists and medical doctors. However, these adhesives have seldom been tested in clinically demanding surgeries. Here we demonstrate adhesive anastomosis in organ transplantation. Anastomosis is commonly conducted by dense sutures and takes a long time, during which all the vessels are occluded. Prolonged occlusion may damage organs and even cause death. We formulate a tough, biocompatible, bioabsorbable adhesive that can sustain tissue tension and pressurized flow. We expose the endothelial surface of vessels onto a gasket, press two endothelial surfaces to the adhesive using a pair of magnetic rings, and reopen the bloodstream immediately. The time for adhesive anastomosis is shortened compared to the time for sutured anastomosis. We have achieved adhesive anastomosis of a great vein in transplanting the liver of a pig. After the surgery, the adhesive is absorbed, the vein heals, and the pig lives for over one month.

1. Introduction

Efforts have long been made to replace sutures with adhesives in surgical procedures, including wound dressing [1,2], hemostasis [3,4], gastrointestinal surgeries [5], and microvascular anastomoses [6]. Adhesives have also been applied for clinically demanding surgeries such as nerve anastomosis and heart-lung transplantations for decades. In nerve anastomosis, the adhesives are applied on the injured neurons with mechanical fixation [7], or work as the tissue scaffold [8,9] to help the neuron regeneration. While the nerve anastomosis does not require a strong adhesion, because the anastomosed nerve will not sustain a large mechanical load such as blood pressure [9,10]. In heart-lung transplantations, the vessels are always anastomosed by suture firstly, and then the adhesive is applied on the periphery of the vessel [11–13]. The adhesives are always used to reduce blood loss and help the suture area to regenerate, which cannot anastomose the vessels together directly due to their low adhesion strength [14–16].

Adhesive anastomosis, however, has yet been demonstrated for organ transplantation. Since 1954, millions of lives have been saved by transplanting organs, including kidneys, livers, hearts, lungs, pancreas, and bowels [17–19]. To transplant an organ, all the affiliated main vessels of the recipient are occluded. The surgeon clamps the vessels, pulls the two ends of the vessels together by threads, and sews a circle of stitches (Fig. 1A) [20,21]. The stitches must be dense enough to prevent bleeding, so that the vessels must be clamped for a long time. During a transplantation of liver, for example, three great veins are occluded,

Peer review under responsibility of KeAi Communications Co., Ltd.
* Corresponding author.
** Corresponding author.
*** Corresponding author.
E-mail addresses: suo@seas.harvard.edu (Z. Suo), tangjd@mail.xjtu.edu.cn (J. Tang), luyi169@xjtu.edu.cn (Y. Lv).
[1] These authors contributed equally to this work.

https://doi.org/10.1016/j.bioactmat.2021.11.003
Received 26 August 2021; Received in revised form 19 October 2021; Accepted 1 November 2021

which blocks the blood to flow from the lower part of the body to the heart (Fig. 1B). Even among skilled surgeons of liver transplantation, the surgery is still time consuming, and the occlusion takes about 45 min, which has not been shortened for decades [22]. Prolonged occlusion may cause ischemia, congestion, systemic inflammatory response syndrome, and multi-organ dysfunction [23].

Here we demonstrate adhesive anastomosis for organ transplantation (Fig. 1C, Video S1). After occlusion, we load a magnetic ring on each end of a vessel, and evert the vessel onto a gasket (Video S2). The endothelial surfaces of the two vessels are glued to a ring of a tough hydrogel. The magnetic rings then press the endothelial surfaces and the hydrogel into tight contact, after which the bloodstream is reopened immediately. When the endothelial surfaces and the hydrogel form strong adhesion, the magnetic rings are removed. The duration of occlusion is set by the time needed before magnetic compression, not by the time needed for adhesion. The eversion of the donor vessel onto a gasket is independent of the occlusion of the recipient vessel, so that the time of each anastomosis is set mainly by the eversion of the recipient vessel. The hydrogel adhesive is strong enough to sustain tissue tension and blood pressure. We show that the hydrogel has negligible cytotoxicity and immune response. We implant the hydrogel in the thigh of a rat, and show that the tissues absorb the hydrogel and heal well. We demonstrate the magnet-assisted adhesive anastomosis in rabbits, as well as in the transplantation of the liver of a pig.

Supplementary data related to this article can be found at https://doi.org/10.1016/j.bioactmat.2021.11.003.

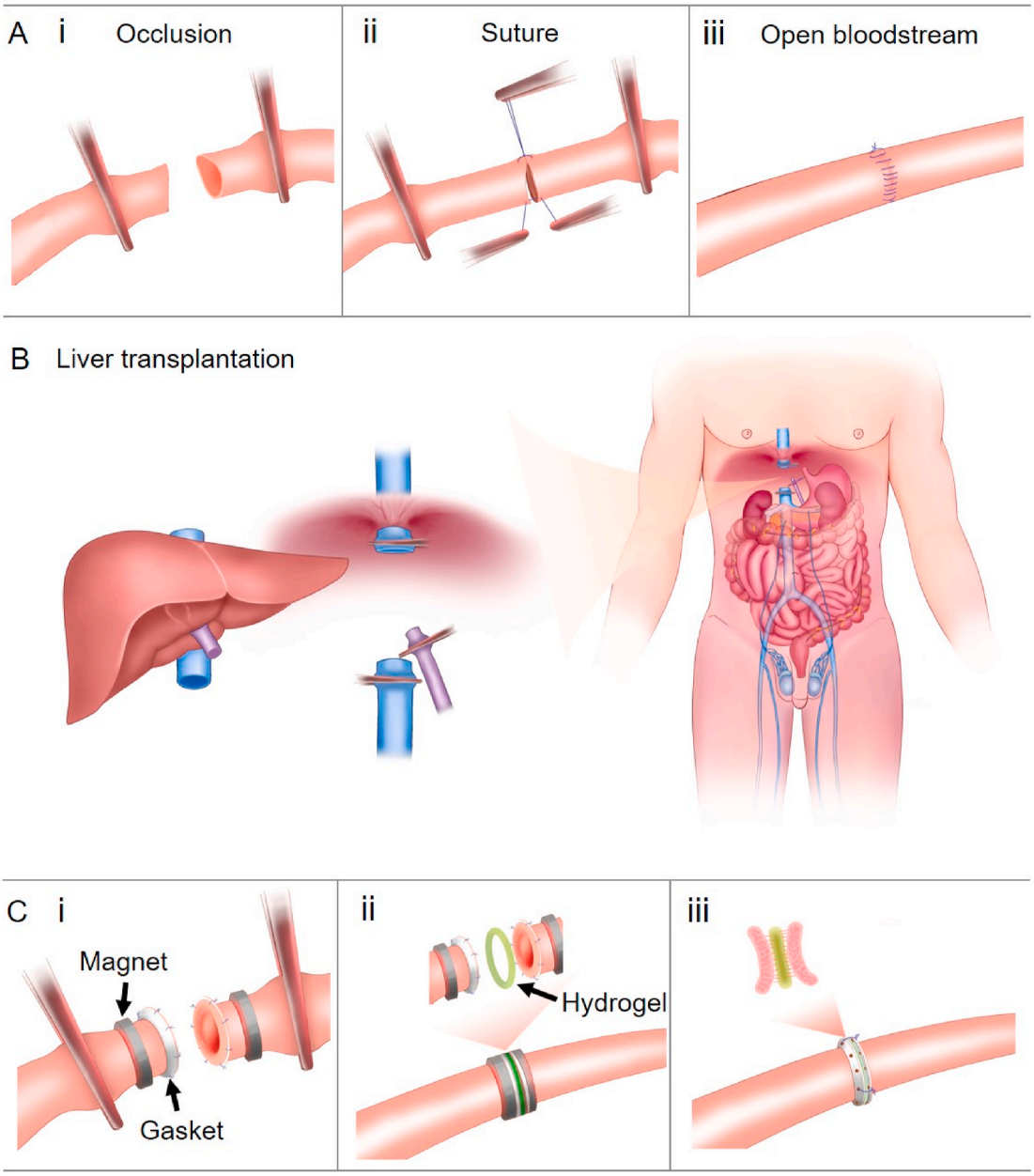

Fig. 1. Vascular anastomosis during organ transplantation. (**A**) Anastomosis by suture proceeds as follows. (i) The vessels are clamped. (ii) The ends of the two vessels are pulled together with threads. (iii) The threads are sewed into a circle of dense stitches. (**B**) In transplanting a liver, three great veins are occluded, which stops blood flowing back to the heart from the lower part of the body. (**C**) A magnet-assisted adhesive anastomosis proceeds as follows. (i) The vessels are occluded, and a magnetic ring is loaded onto each end of a vessel, which is then everted onto a gasket. (ii) The endothelial surfaces of two vessels are glued to a hydrogel ring and pressed by the magnetic rings, after which the bloodstream is reopened immediately. (iii) When strong adhesion sets in, the magnetic rings are removed.

2. Results and discussion

Adhesive anastomosis has never been demonstrated for organ transplantation before. To demonstrate this potential, we continue the recent development of tough, adhesive, bioabsorbable hydrogels. The mechanisms for tissue adhesion and hydrogel degradation are illustrated in Fig. 2.

The strength and toughness of the hydrogel come from the synergy of the two interpenetrating polymer networks: a polyacrylamide network of covalent crosslinks, and an alginate network of calcium-ion crosslinks [24]. The glue is an aqueous solution of chitosan, 1-ethyl-3-(3-(dimethylamino)propyl) carbodiimide hydrochloride (EDC), and N-hydroxysulfosuccinimide sodium salt (NHS) [15]. The amine groups on chitosan, in the presence of EDC and NHS, form peptide bonds with carboxyl groups on a tissue and on the alginate—that is, the chitosan acts as bridging polymers between the tissue and the hydrogel. During peel, the strong peptide bonds cause the calcium-ion crosslinks in the interior of the hydrogel to unzip, leading to high adhesion toughness [15,25]. The polyacrylamide network is crosslinked by disulfide bonds [26]. Disulfide bond is a typical dynamic covalent bond, which can dissociate into thiol group under external stimulus (e.g., solvent, pH, and UV light), and reform by oxidation. It is also an important component of the secondary and tertiary structure of proteins, and receives significant attention in the biomedical field [27–30]. Surrounded by living tissues, the alginate network dissociates as the calcium ions exchange with sodium ions [31], and the polyacrylamide network dissociates as the disulfide crosslinks react with amino acids (e.g., cysteine) [26,32]. Consequently, the hydrogel is tough, adhesive, and bioabsorbable. This paper focuses on the use of this hydrogel in vascular anastomosis. We have characterized the degradation kinetics and durability of adhesion for this tough hydrogel through *in vitro* tests in our previous work [32]. The tough hydrogel can degrade in the mixture of PBS buffer solution and cysteine, and its volume and compressive strength can decrease to almost zero. The adhesion energy would decline substantially after being submerged in the mixture solution, as a result of the degradation of the hydrogel. The *in vivo* test on the degradation of the hydrogel is needed, which will be shown later.

Anastomosis for organ transplantation must sustain tissue tension and enable the vessel to heal, as well as prevent bleeding, thrombosis, and stenosis [20]. These requirements cannot be fulfilled by commercial tissue adhesives, such as cyanoacrylate, fibrin, gelatin, and polyethylene glycol. We compare these commercial tissue adhesives to the tough hydrogel adhesive using lap shear (Fig. 3A) and peel tests (Fig. 3B). Cyanoacrylate is applied to the endothelium of a vessel, and another vessel is compressed on it and held for ~10 min. The PEG glue is similarly used by painting the mixture of A and B quickly on the vessel. The gelatin powder with a high polymer concentration (40 wt%) is dissolved in hot deionized water (90 °C), and 0.1 wt% EDC and 0.1 wt% NHS are added. We paint the hot gelatin solution to the endothelium of a vessel and compress it for ~10 min. Cyanoacrylate cures into a polymer glass, which is much stiffer than vessels and does not enable vessels to heal [33,34]. Adhesion strength and toughness of cyanoacrylate is low, probably because the monomers polymerize instantly on the wet aorta surfaces, and the polycyanoacrylate fails to interlock with the tissue. PEG and gelatin also show low adhesion strength and toughness, because the materials themselves are weak [14,35,36]. By contrast, the tough hydrogel adhesive has high adhesion strength (~56 ± 8 kPa) and toughness (~368 ± 26 J/m^2). The hysteresis of tough hydrogel enhances the adhesion toughness (Fig. S1).

Strong adhesion is established after 10 min (Fig. 3C). The surgeon may desire that strong adhesion forms, say, between tens of seconds to a minute, without compression. This requirement markedly narrows the

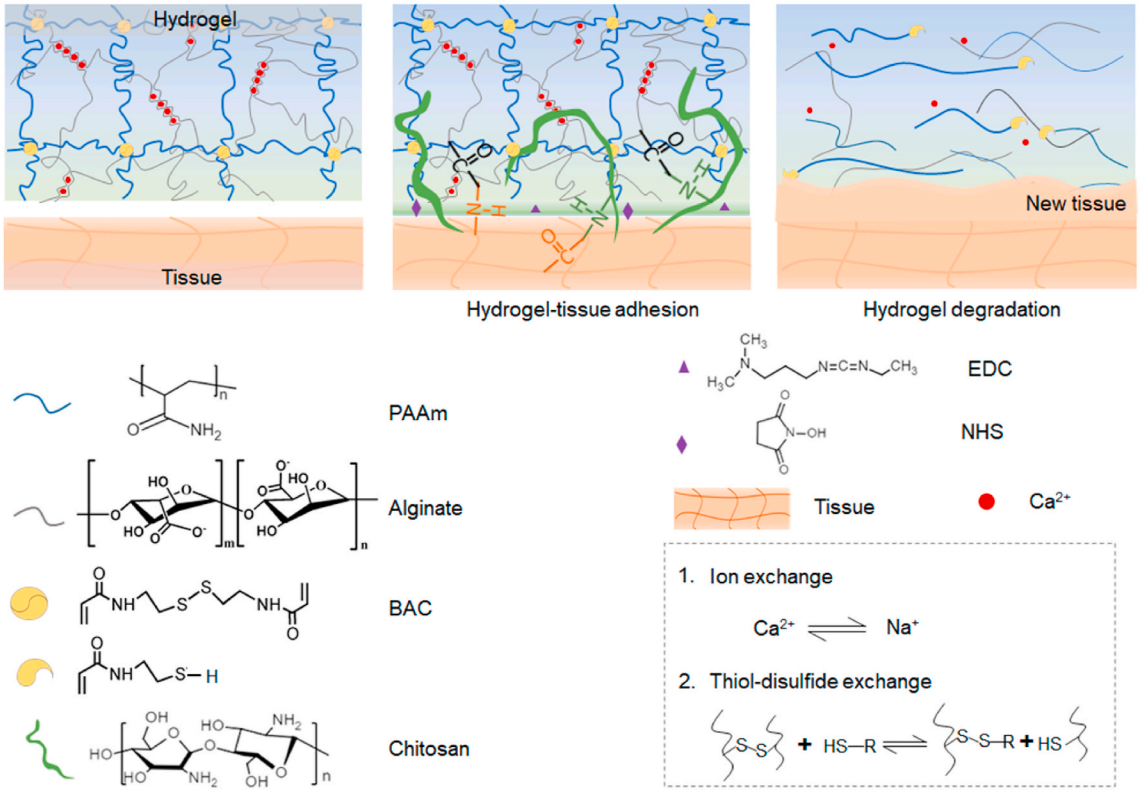

Fig. 2. The bioabsorbable hydrogel and bioconjugation glue. The hydrogel has two polymer networks: an alginate network crosslinked by calcium ions, and a polyacrylamide network crosslinked by disulfide. The glue is an aqueous solution of chitosan, 1-(3-Dimethylaminopropyl)-3-ethylcarbodiimide hydrochloride (EDC), and N-Hydroxysuccinimide (NHS). To adhere, the glue is spread between the hydrogel and the tissue, then EDC and NHS enable the amine groups on the chitosan chains to react with the carboxyl groups on the alginate and on the tissue. To degrade, the sodium ions in the environment exchange with calcium ions to uncrosslink the alginate network, and cysteine in the surroundings reacts with the disulfide to uncrosslink the polyacrylamide network.

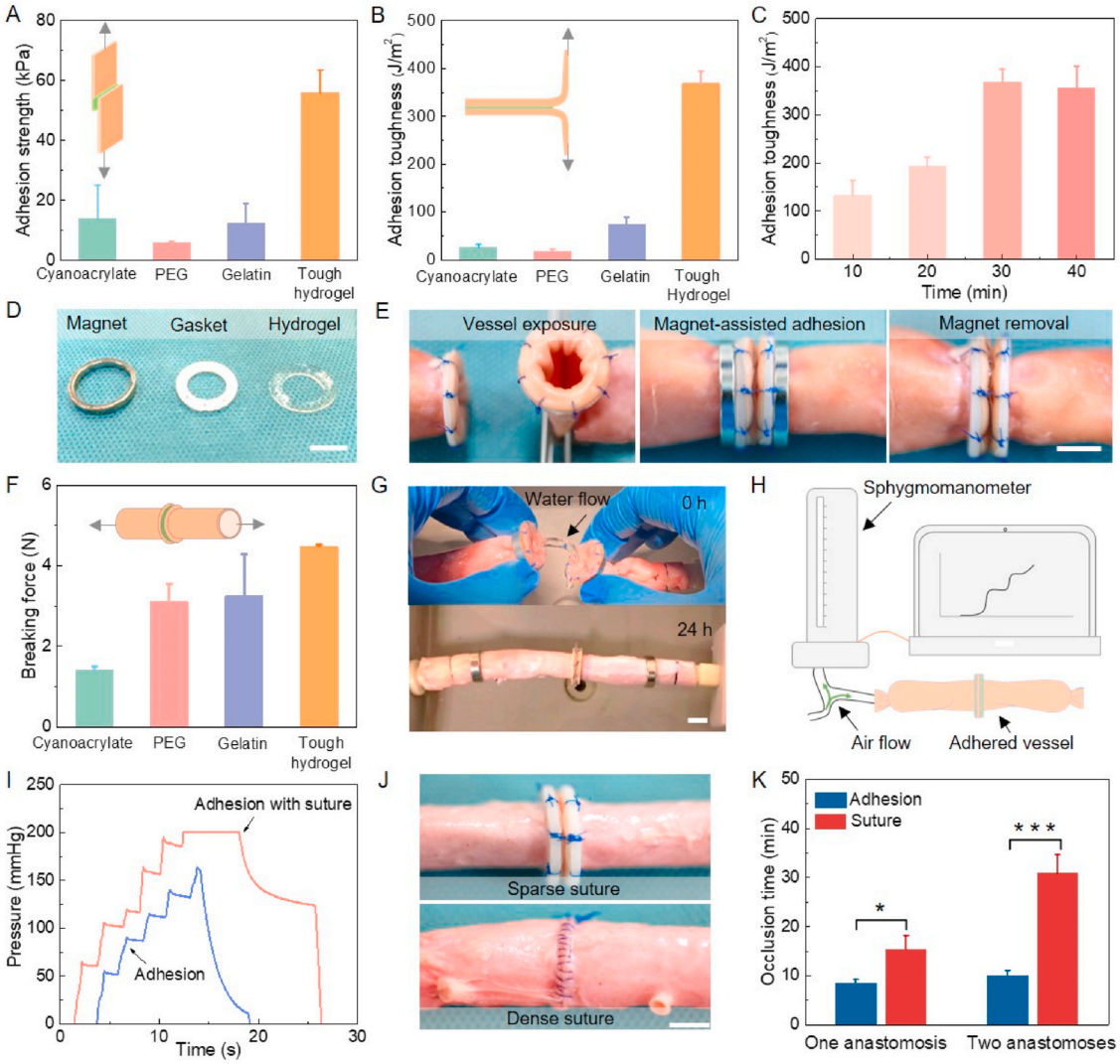

Fig. 3. Properties of adhesives and magnet-assisted adhesive anastomosis *in vitro*. (A) Strength and (**B**) toughness of various adhesives bonding to porcine aortas. (**C**) Adhesion toughness of the tough hydrogel as a function of time. (**D**) Photographs of the magnet, gasket, and hydrogel. (**E**) Three steps of a magnet-assisted adhesive anastomosis *in vitro*. (**F**) The breaking force of the vessels adhered using various adhesives. (**G**) The adhered vessels can sustain water flow of pressure ~50 mm Hg for 24 h. (**H**) The setup for the burst pressure test. An adhered vessel is clamped at one end, and air is pumped into the vessel from the other end. (**I**) The adhered vessel can endure an air pressure ~160 mm Hg without suture, and ~200 mm Hg with sparse sutures. (**J**) Sparse suture in adhesive anastomosis and dense suture in conventional anastomosis. (**K**) Comparison of the occlusion time for adhesive anastomosis and conventional sutured anastomosis. In connecting two vessel ends, one anastomosis is operated. In transplanting a vessel graft, two anastomoses are operated.

path for the development of tissue adhesives. Living vessels are usually under tension, which requires compression no matter how fast an adhesion is. The magnetic rings press the two vessel ends and the hydrogel into tight contact. We carry out the magnet-assisted adhesive anastomosis *in vitro*, using rings of magnet, gasket, and hydrogel (Fig. 3D). Fig. 3E shows the exposed vessel, magnet-assisted adhesion, and adhered vessels after the magnets are removed. Exposure of the vessel by the gasket provides a smooth endothelial surface, and is crucial to successful anastomosis (Fig. S2). We pull the adhered vessels and measure the breaking force. The breaking force of the tough hydrogel is more than twice that of cyanoacrylate, and the adhered vessel can bear a moderate stretch (Fig. 3F). We design a water circulation setup to simulate blood circulation (Fig. S3, Video S3). The adhered vessels can sustain 24 h of water circulation under a pressure of ~50 mm Hg, which is much higher than the normal blood pressure in veins ~10 mm Hg (Fig. 3G). As a comparison, we also use the setup to test gelatin for adhesive anastomosis. The gelatin painted on the exposed vessel ends flows and clogs the vessel. We further use the magnetic rings to press the vessel ends and then paint gelatin around the contact, but the gelatin swells excessively, leading to rupture and leakage (Fig. S4).

Supplementary data related to this article can be found at https://doi.org/10.1016/j.bioactmat.2021.11.003.

We also subject the tough hydrogel to a burst test using compressed air (Fig. 3H). The maximum pressure for the adhesive anastomosis is ~160 mm Hg (Fig. 3I, Video S4). When sparse sutures (2 sutures) are used to tie the two gasket rings, the maximum pressure reaches 200 mm Hg (Video S5). When we test the vessel anastomosed by dense suture, air leaks between stitches. Fig. 3J shows the photograph of the dense suture and sparse suture. For a single anastomosis, the occlusion time is 8.51 ± 0.73 min for adhesive anastomosis, and is 15.28 ± 2.86 min for dense suture in case of blood leakage. A vascular transplantation requires two anastomoses, and the occlusion time is 10.03 ± 1.14 min for adhesive anastomosis, and is 30.79 ± 3.82 min for dense suture (Fig. 3K). Fig. S5 shows the photograph for the vascular transplantation by adhesive and sutured anastomosis. The above tests demonstrate the effectiveness of the adhesive anastomosis *in vitro*.

Supplementary data related to this article can be found at https://doi.org/10.1016/j.bioactmat.2021.11.003.

Next, we show that the hydrogel has negligible cytotoxicity to the human umbilical vein endothelial cells (HUVECs). A mass of the hydrogel (mg) is submerged in an amount of a cell culture medium (mL). After 24 h, the hydrogel is removed, and the medium is used to culture the HUVECs for 72 h, followed by immunofluorescence imaging. The survival of cells in the hydrogel-treated medium is comparable to that of the cells in the control medium (Fig. 4A and B). We also culture the HUVECs on a piece of the hydrogel submerged in the cell culture medium, and observe negligible cytotoxicity for 7 days (Fig. S6).

To study the effect of the hydrogel on the immune response, we submerge various amounts of the hydrogel in a cell culture medium, which is then used to culture the peripheral blood mononuclear cells (PBMCs). The mRNA levels of inflammatory cytokines, including TNF-α and IL-6, do not increase after hydrogel treated (Fig. 4C). These results suggest that the hydrogel only induces negligible inflammatory response to the human blood cells.

We investigate *in vivo* biocompatibility of the hydrogel implanted under the skin on the back of rats (Fig. 4D). At various times after the implantation, we obtain samples of subcutaneous tissues. The hydrogel is absorbed after 3 weeks of implantation. The histology of the tissue at 1 week shows a mild inflammatory response, with infiltration of macrophages, lymphocytes, and neutrophils. Also observed is the formation of granulation tissues, consisting of fibroblasts, collagen, and thin-walled capillary. We do not observe any eosinophilic response or the necrosis of the overlying skeletal muscle. The inflammatory response diminishes with time, and disappears after 4 weeks. The quantitative result of the subcutaneous inflammation further validates the observation (Fig. 4E).

The mild inflammatory response may result from the tough alginate-PAAm hydrogel and chitosan-based glue (with EDC and NHS). While it has been previously validated that the alginate-PAAm hydrogel has negligible cytotoxicity and causes minimal inflammation *in vivo* [15,31]. As for EDC and NHS, they are widely used for the coupling of $-NH_2$ and –COOH in various fields, and considered to be acceptable for biological treatment [37,38]. In our study, the dosage of EDC and NHS is extremely small, where each agent only takes 0.24 wt% in the glue and ~0.1 mg for a vessel junction, which is considered to be safe.

We then cut the muscle of a thigh of rat, implant the hydrogel, and watch the muscle absorb the hydrogel and heal (Fig. 4F and G). At 0 day, the boundary between the hydrogel and the muscle is clearly observed. At 1 week, the hydrogel fragments and is partially absorbed, and the granulation tissue and inflammatory cells grow into the hydrogel. Subsequently, the injured muscle is gradually repaired by fibrous tissues without an obvious inflammatory response. At 4 weeks, the implanted hydrogel is absorbed and the muscle heals. The quantitative result shows that the area of hydrogel decreases by ~50% within 7 days and degrade almost completely within ~28 days *in vivo* (Fig. 4G). We further test the magnet-assisted adhesive anastomosis in rabbits to validate its effectiveness *in vivo* (Fig. S7).

We demonstrate the magnet-assisted adhesive anastomosis in transplanting livers of pigs. General anesthesia and tracheal intubation

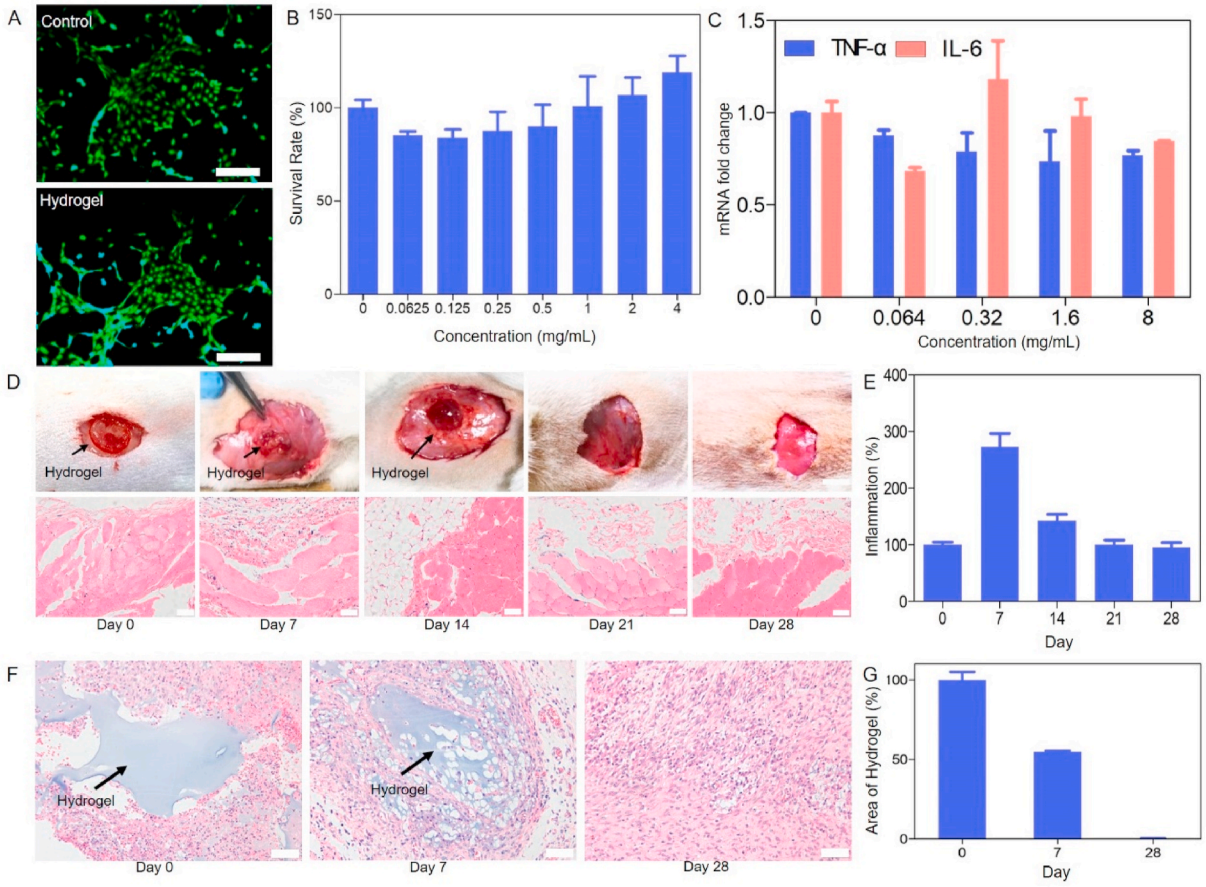

Fig. 4. Cytotoxicity, biocompatibility, and degradability of tough hydrogel adhesive. (**A**) Immunofluorescence image of the HUVECs in the control medium is comparable to that of the HUVECs in the hydrogel-submerged medium. The hydrogel to medium ratio is 4 mg/mL. Scale bar, 200 μm. (**B**) Survival rate of the HUVECs as a function of ratio of the hydrogel to the medium. (**C**) Ratio of mRNA of the peripheral blood mononuclear cells (PBMCs) in a hydrogel-submerged medium to the PBMCs in the control medium. (**D**) The hydrogel is implanted under the skin on the back of a rat model. Over time, the inflammation is negligible and the hydrogel is absorbed (scale bar, 50 μm). (**E**) Quantification of the subcutaneous inflammation. (**F**) In a rat model, the muscle of a thigh is cut, and the hydrogel is implanted. The hydrogel is absorbed and the muscle heals in 4 weeks (scale bar, 50 μm). (**G**) Quantification of the hydrogel area during degradation.

are applied to a pair of pigs. Two pigs are used for animal models. One of them is the liver donor and the other is the recipient. Transplanting a liver requires anastomoses of three great veins. We use sutures for the anastomoses of the suprahepatic vena cava and portal vein, and use magnet-assisted adhesive anastomosis for the infrahepatic vena cava (Fig. 5A). The adhesive anastomosis includes the following main steps (Fig. 5B). We resect the liver from the donor, place a magnetic ring on its infrahepatic vena cava, evert the vessel onto a gasket, and glue the exposed endothelial surface to a hydrogel ring. We then clamp the three great veins and the hepatic artery of the recipient, resect its liver, place a magnetic ring on the infrahepatic vena cava, and evert the vessel onto a gasket. We glue the exposed endothelial surface of the recipient to the hydrogel ring on the endothelial surface of the donor. When all the three great veins are anastomosed, we unclamp them immediately. We then anastomose the hepatic artery and the bile duct by suture. After strong adhesion sets in, we remove the magnetic rings, and close the abdomen. The ultrasonography indicates that blood flows in the vessel (Fig. 5C). The pig recovers well after surgery (Video S6). The pig receives an anticoagulant drug daily (warfarin, 2.5 mg/day). In one week after the surgery, the liver function recovers to the normal range (Fig. 5D). The pig lives for 38 days, and dies of suppurative cholangitis. This cause of death is not directly related to the anastomosis. Autopsy shows that the infrahepatic vena cava remains open with smooth endothelium, the hydrogel is absorbed, and the vascular tissues heal (Fig. 5E–G). The images of scanning electron microscopy and hematoxylin-eosin staining further confirm the healing of the vascular tissues (Fig. 5H). We also attempt the magnet-assisted adhesive anastomosis of all the three great veins, and describe the surgery in Supplementary Information (Fig. S8, Video S7).

Supplementary data related to this article can be found at https://doi.org/10.1016/j.bioactmat.2021.11.003.

3. Conclusions

We have reported the first case in achieving adhesive anastomosis of a main vessel in organ transplantation. After the surgery, the pig lives, the hydrogel is absorbed, and the vein heals. It is well known that vascular anastomosis by suture has become the cornerstone and standard clinical practice of vascular, cardiovascular and transplant surgery, since Alexis Carrel invented this technique in 1902, and won the Nobel Prize in 1912 [6]. As suturing is very difficult and time-consuming, many alternative methods have been proposed, such as vascular

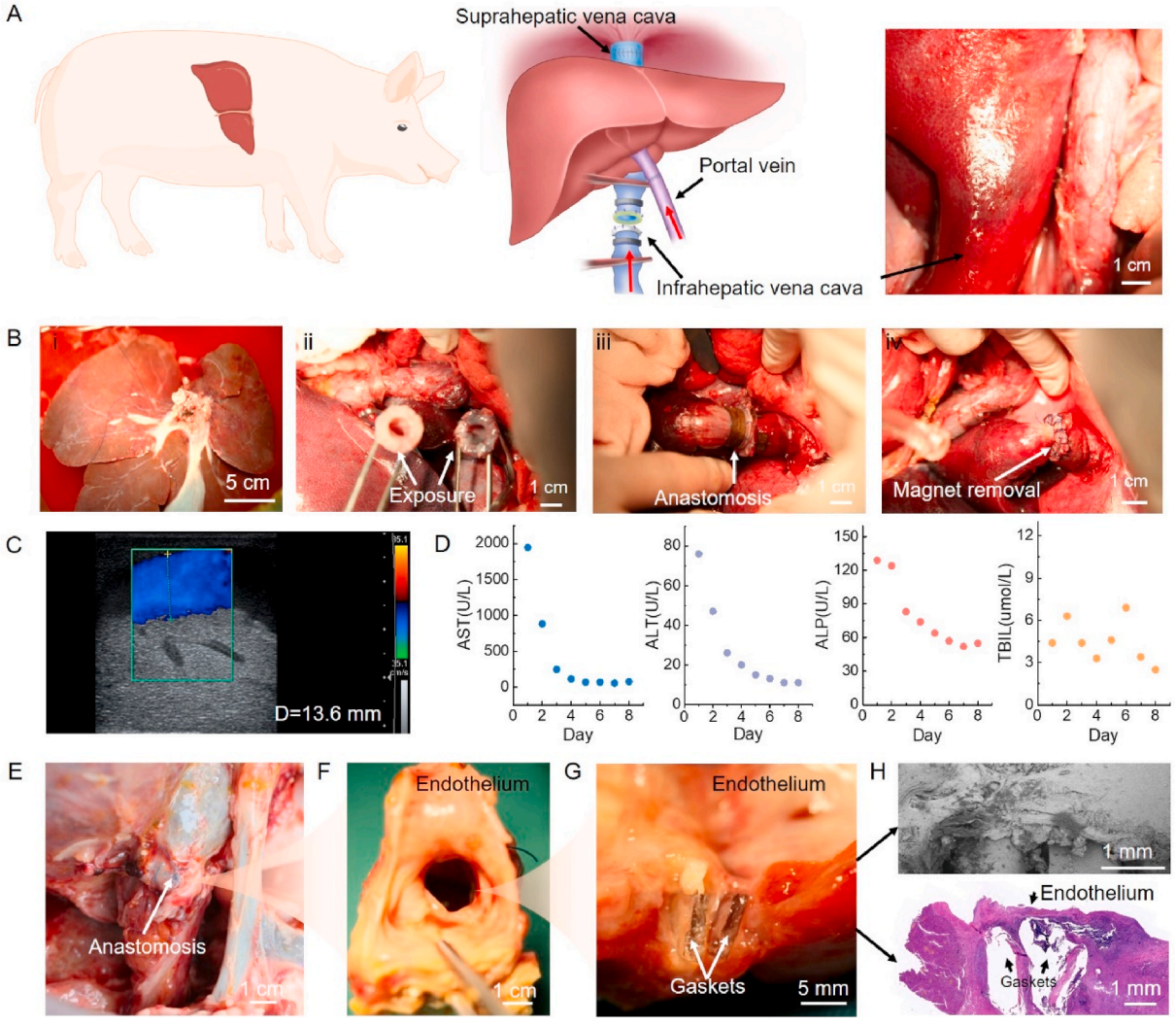

Fig. 5. Magnet-assisted adhesive anastomosis in transplanting liver of a pig. (**A**) Transplanting a liver requires the anastomoses of three great veins. (**B**) (i) donor liver, (ii) exposure of infrahepatic vena cava, (iii) magnet-assisted adhesive anastomosis, and (iv) removal of magnetic rings. (**C**) Ultrasound Doppler image of bloodstream through the adhered vessel. (**D**) Liver function indicators: AST, ALT, ALP, and TBIL. (**E**) Autopsy is conducted after 38 days of liver transplantation. Photo of the adhesive anastomosis. (**F**) A cross-section view of the anastomosed vessel. (**G**) A longitudinal section of the two gaskets. (**H**) Images of the scanning electron microscopy and hematoxylin-eosin staining.

closure device [39], laser welding [40], poloxamer stent [6] and negative pressure device [41]. Unfortunately, suturing anastomosis is still the only method to anastomose vessels in clinical organ transplantation. Our research is designed as an explorative research to prove that adhesive could replace suture in vascular anastomosis. This technique is still not mature at the current stage, while it may be a beneficial attempt in this field. Adhesive anastomosis for organ transplantation opens a frontier for bioengineering and medicine. Work is ongoing to further develop adhesive anastomosis to shorten the time of occlusion during liver transplantation. It is also hoped that adhesive anastomosis will be soon explored in the transplantation of other organs, such as the lung, kidney, and heart.

4. Material and methods

4.1. Materials

All chemicals were used as purchased without further purification. Acrylamide, sodium alginate, ammonium persulfate, calcium sulfate; 1-ethyl-3-(3-(dimethylamino) propyl) carbodiimide hydrochloride (EDC), N-hydroxysuccinimide (NHS), and 4-morpholineethanesulfonic acid (MES hydrate) were purchased from Aladdin®. N, N, N′, N′-tetramethylethylenediamine (TEMED), N, N′- bis (acryloyl)cystamine, gelatin (300 g bloom), and chitosan (Medium viscosity) were purchased from Sigma-Aldrich. Heparin sodium (12,500 units) was purchased from SPH No.1 Biochemical & Pharmaceutical Co., Ltd. The cyanoacrylate was purchased from Guangzhou Baiyun Medical Glue Co., Ltd. The PEG glue was purchased from Shandong Saikesaisi Biotechnology Co., Ltd. The glutaraldehyde was purchased from Tianjin Beilian Chemical Co., Ltd.

4.2. Synthesis of the hydrogel

The hydrogel was synthesized using a method similar to the previously reported work [26,32]. Briefly, acrylamide (3.6 g), sodium alginate (0.6 g), and N, N′-bis(acryloyl)cystamine (0.0132 g) were dissolved in deionized water (28 g) at low temperature (~4 °C). Ammonium persulfate (0.057 g) and heparin sodium (1 mL) were added and mixed to form a uniform solution. TEMED (30 μL) and calcium sulfate ($CaSO_4$, 1050 μL, 0.1135 g/mL) were added and stirred quickly to form a slurry. The slurry was cured inside two pieces of glass with a spacer (500 μm) at 50 °C for 2 h and then cooled down to room temperature overnight. Hydrogels with different concentration ratios of $CaSO_4$ to alginate were fabricated by adjusting the dosage of $CaSO_4$ (0, 1575 μL, 2100 μL and 3150 μL).

4.3. Preparation of chitosan solution

MES (0.976 g) was dissolved into deionized water (50 g). Chitosan powder (1 g) was added and stirred overnight on a magnetic stirrer. A uniform thick solution was formed.

4.4. Mechanical tests

The vessels were cut into a rectangular shape. Different adhesives were used as follows. Cyanoacrylate was applied on the endothelium of a vessel, and another vessel was compressed on it and held for ~10 min. The PEG glue was used by painting the mixture of A and B quickly on the endothelium of a vessel, and another vessel was compressed on it and held for ~10 min. The gelatin powder (concentration, 40 wt%) was dissolved in deionized water (90 °C), and 0.1 wt% EDC and 0.1 wt% NHS were added. We painted the hot gelatin solution to the endothelium of a vessel and compress it for ~10 min. For tough hydrogel adhesion, the chitosan solution with 0.24 wt% EDC and 0.24 wt% NHS was painted on the inner surface of a vessel, the tough hydrogel was applied between the two pieces of vessels, and the adhered vessels were compressed gently with a piece of glass plate. For the adhesion of crosslinked chitosan, the chitosan solution (2 wt%) was mixed with glutaraldehyde (20 μL/mL) with the volume ratio of 10:1, and applied between two vessels. For the adhesion of only chitosan solution, the chitosan solution (2 wt% and 4 wt%) with 0.24 wt% EDC and 0.24 wt% NHS was painted on the endothelium of a vessel, and another vessel was compressed on it and held for 1 h.

The mechanical tests were performed on a universal mechanical test system (AGS-X with 100 N sensor). The loading speed was 50 mm/min. For the lap shear test (ASTM F2255), we measured the maximum force during stretch, and the adhesion strength was calculated by dividing the maximum force by the adhesion area. For the peel test (ASTM F2256), we measured the average value of stable peel force and calculated the adhesion toughness as twice of the stable peel force divided by the width of the specimen. For the breaking force test of the end-to-end adhered vessel, two vessels were glued together by different adhesives and then stretched on the test machine. We recorded the breaking force as the maximum value on the force-displacement curve.

4.5. Burst pressure test

The burst pressure tests were performed underwater by applying air pressure until leakage was observed (Fig. 3H). Briefly, two vessels were glued together using various adhesives. With one end closed by a wire, the other end connected to a pressure supplying system (Mercurial sphygmomanometer, Yuyue Medical Equipment and Supply Co., Ltd.). The pressure was continuously recorded by PT-102 blood pressure transducer and BL-420F biological signal acquisition and analysis system (Techman Software Co., Ltd).

4.6. In vitro anastomosis

We performed *in vitro* anastomosis to show the procedure and the adhesion property of tough hydrogels with vessels in water flow (Fig. S3). Two vessels were fixed on a water circulation setup simulating the blood circulation. Each end of the vessel was everted onto a gasket to expose the endothelium. After the chitosan solution (with 0.24 wt%, EDC and 0.24 wt% NHS) was painted on the exposed endothelium, a hydrogel ring was placed onto it. Magnetic rings then compressed the adhesion area evenly. The magnetic rings were removed after 20 min.

4.7. Cell culture

Human umbilical vein endothelial cells (HUVEC) were purchased from the American Type Culture Collection, and were cultured in an endothelial cell medium supplemented with 10% fetal bovine serum (FBS) and 1% penicillin/streptomycin (Gibco; Thermo Fisher Scientific, Inc.) at 37 °C with 5% CO_2.

Cell viability was determined with a Cell Counting Kit-8 (CCK-8) assay (Dojindo, Tokyo, Japan). HUVEC cells were seeded in 96-well plates overnight and then treated with various concentrations of extracting liquid from hydrogel. After 72 h, the cell viability was measured by CCK-8 assays.

4.8. Cell fluorescence imaging

Human Umbilical Vein Endothelial (HUVEC) cells were transfected with lentivirus with Green fluorescent protein (GFP) flag. The HUVECs with GFP were cultured by cell medium and finally observed by fluorescence microscope at different times.

4.9. Isolation of peripheral blood mononuclear cell (PBMC)

The fresh PBMC was isolated from healthy donors. Then the blood samples were used for the density gradient centrifugation. PBMCs were seeded in six-well plates at a density of 1 × 107 cells per well in 2 mL of serum-free AIM V medium containing various concentrations of gel

extraction, and incubated at 37 °C with 5% CO_2 for 4 h.

4.10. RNA extraction, quantitative and relative real-time PCR (qRT-PCR)

RNA was extracted by using TRIzol® reagent (Ambion-Life Technologies, Carlsbad, CA, USA) followed by the chloroform: phenol method as described previously. Five hundred ng of total RNA was reverse transcribed using the high capacity cDNA Reverse Transcription Kit (TaKaRa, Japan), and qRT-PCR was carried out using the TaKaRa TB Green™ Premix Ex Taq™ II Kit (TaKaRa, Japan), according to the manufacturer's instructions. The endogenous control was GAPDH. The primer sequences used were shown as follows:

TNFα forward: 5′-CTCTTCTGCCTGCTGCACTTTG-3'; reverse: 5′-ATGGGCTACAGGCTTGTCACT-3';

IFN-γ forward: 5′-GAGTGTGGAGACCATCAAGGAAG-3′, reverse: 5′-TGCTTTGCGTTGGACATTCAAGTC-3';

IL-6 forward: 5′-AGACAGCCACTCACCTCTTCAG-3′, reverse: 5′-TTCTGCCAGTGCCTCTTTGCTG-3';

GAPDH forward: 5′-GTCTCCTCTGACTTCAACAGCG-3′, reverse: 5′-ACCACCCTGTTGCTGTAGCCAA-3'.

4.11. In vivo adhesion, biocompatibility, and biodegradability tests

All animal procedures were reviewed and approved by the Institutional Animal Care and Use Committee of Xi'an Jiaotong University Health Science Center. All animals received humane care according to the criteria outlined in the "Guide for the Care and Use of Laboratory Animals."

4.12. In vivo biocompatibility and degradability test

We evaluated the subcutaneous biocompatibility and degradability of the tough hydrogel in a rat model. The hydrogel was cut into small disks of 10 mm in diameter. The rats were anesthetized by intraperitoneal injection of 3% sodium pentobarbital. Two small incisions were made on each rat in the back skin on both sides of the spine. Then the small hydrogel disk was placed in each incision and the incisions were sutured. At a certain time, we took the specimen for H&E staining and took pictures.

4.13. In vivo tissue healing test

We carried out the tissue healing test in a rat model. The hydrogel was cut into strips of 10 mm long and 5 mm wide. The rats were anesthetized by intraperitoneal injection of 3% sodium pentobarbital. We cut the thigh muscle of the rat and placed the hydrogel strip into the incision. Then we sutured the incisions. At a certain time, we took the specimen for H&E staining and took pictures.

4.14. In vivo vascular anastomosis experiment

We carried out the vascular anastomosis experiment in a rabbit model (Fig. S7). The rabbit was anesthetized by intravenous injection of 3% sodium pentobarbital. We cut the abdominal cavity of the rabbit, freed the inferior vena cava (IVC), clamped the IVC, and cut it. Then we exposed the vascular endothelium on gaskets and anastomosed two vascular ends by magnet-assisted adhesive anastomosis. After the magnetic rings compressed the two endothelial surfaces to the hydrogel, the bloodstream was opened immediately. After 20 min, we removed the magnetic rings and sutured the abdomen.

4.15. In vivo liver transplantation experiment

We carried out the liver transplantation in a porcine model. The liver graft was obtained from pigs sacrificed for other experiments. Before surgery, we exposed the end of the infrahepatic vena cava in liver graft by a plastic gasket and adhered the endothelium to the hydrogel. We used the intravenous injection of 3% sodium pentobarbital to induce anesthesia and inhalation of isoflurane to maintain intraoperative anesthesia. We cut the abdominal cavity of the pig and freed the pig liver and its vessels. We used suture to anastomose suprahepatic vena cava and portal vein, while used magnet-assisted adhesive anastomosis to anastomose infrahepatic vena cava. After that, we opened the bloodstream and removed the magnetic rings. Finally, we sutured the abdomen.

4.16. Animal anastomotic patency examination

Ultrasound assessment of anastomotic patency was performed using a Philips 5500 ultrasound system (Philips Medical, Andover, MA) with a 7 MHz transducer. The angiographic image was used to show the anastomotic patency (Innova 4100 Angiographic Imaging System, Modular Devices Inc, IN).

4.17. Liver function examination

The animal blood samples were collected every day in the first 8 days after the surgery. Blood was collected into sterile evacuated tubes containing coagulant. After centrifugation (4500 rpm for 15 min at 4 °C), the supernatant plasma was collected and sent for analysis. Liver function indicators, including AST, ALT, ALP and TBIL, were detected.

4.18. Histologic analysis

Vascular tissues were embedded in paraffin. 4-mm-thick cross-sections were longitudinally cut through the anastomotic stoma with both proximal and distal ends adjacent to the anastomoses. Longitudinal sections of anastomoses were stained with hematoxylin-eosin and examined under a bright-field microscope.

4.19. Scanning electron microscopy

The specimens were fixed overnight in 1% glutaraldehyde, dehydrated in graded ethanol, and dried in liquid carbon dioxide. They were then sputter-coated with gold-palladium and photographed in a scanning electron microscope (Hitachi, TM-1000).

4.20. Quantification of descriptive pictures

The descriptive pictures in Fig. 4D and F and Fig. S6 were quantified by Image J software.

CRediT authorship contribution statement

Kang Liu: contribute equally to this work, conducted the in vitro test and mechanical test, did a subcutaneous implantation test in a rat model. **Hang Yang:** contribute equally to this work, conducted the in vitro test and mechanical test, prepared the hydrogels. **Gaobo Huang:** contribute equally to this work, conducted the in vitro test and mechanical test. **Aihua Shi:** manufactured the gaskets and magnets. **Qiang Lu:** helped with animal experiments. **Shanpei Wang:** helped with animal experiments. **Wei Qiao:** helped with animal experiments. **Haohua Wang:** helped with animal experiments. **Mengyun Ke:** did cell culture and analysis. **Hongfan Ding:** helped with animal experiments. **Tao Li:** helped with animal experiments. **Yanchao Zhang:** helped with animal experiments. **Jiawei Yu:** helped with animal experiments. **Bingyi Ren:** helped with animal experiments. **Rongfeng Wang:** helped with animal experiments. **Kailing Wang:** helped with animal experiments. **Hui Feng:** helped with animal experiments. **Zhigang Suo:** designed the research, All authors contribute to the writing of the paper. **Jingda Tang:** designed the research, All authors contribute to the writing of the

paper. **Yi Lv:** designed the research, All authors contribute to the writing of the paper.

Declaration of competing interest

The authors declare no competing financial interests.

Acknowledgments

This work was supported by grants from the Key R&D Project of Shaanxi Province (No. 2020GXLH-Z-001), the National Key R&D Project of China (No. 2018YFC0115300 and No.2018YFC0115305), the National Natural Science Foundation of China (No. 81727802, 12172272, 11702208, 11820101001), China Postdoctoral Science Foundation (No. BX201700192, 2018M643620). We thank Fengkai Liu for the help of experiment.

Appendix A. Supplementary data

Supplementary data to this article can be found online at https://doi.org/10.1016/j.bioactmat.2021.11.003.

References

[1] J.S. Boateng, K.H. Matthews, H.N.E. Stevens, G.M. Eccleston, Wound healing dressings and drug delivery systems: a review, J. Pharmaceut. Sci. 97 (8) (2008) 2892–2923.
[2] S. Blacklow, J. Li, B. Freedman, M. Zeidi, C. Chen, D. Mooney, Bioinspired mechanically active adhesive dressings to accelerate wound closure, Science advances 5 (7) (2019), eaaw3963.
[3] N. Lang, M.J. Pereira, Y. Lee, I. Friehs, N.V. Vasilyev, E.N. Feins, K. Ablasser, E. D. O'Cearbhaill, C. Xu, A. Fabozzo, R. Padera, S. Wasserman, F. Freudenthal, L. S. Ferreira, R. Langer, J.M. Karp, P.J. del Nido, A blood-resistant surgical glue for minimally invasive repair of vessels and heart defects, Sci. Transl. Med. 6 (218) (2014) 218ra6.
[4] N. Annabi, K. Yue, A. Tamayol, A. Khademhosseini, Elastic sealants for surgical applications, Eur. J. Pharm. Biopharm. 95 (2015) 27–39.
[5] X. Xu, X. Xia, K. Zhang, A. Rai, Z. Li, P. Zhao, K. Wei, L. Zou, B. Yang, W.-K. Wong, Bioadhesive hydrogels demonstrating pH-independent and ultrafast gelation promote gastric ulcer healing in pigs, Sci. Transl. Med. 12 (558) (2020), eaba8014.
[6] E.I. Chang, M.G. Galvez, J.P. Glotzbach, C.D. Hamou, S. El-ftesi, C.T. Rappleye, K.-M. Sommer, J. Rajadas, O.J. Abilez, G.G. Fuller, Vascular anastomosis using controlled phase transitions in poloxamer gels, Nat. Med. 17 (9) (2011) 1147–1152.
[7] A. Narakas, The use of fibrin glue in repair of peripheral nerves, Orthop. Clin. N. Am. 19 (1) (1988) 187–199.
[8] N. Ghane, M.H. Beigi, S. Labbaf, M.H. Nasr-Esfahani, A. Kiani, Design of hydrogel-based scaffolds for the treatment of spinal cord injuries, J. Mater. Chem. B 8 (47) (2020) 10712–10738.
[9] D. Macaya, M. Spector, Injectable hydrogel materials for spinal cord regeneration: a review, Biomed. Mater. 7 (1) (2012), 012001.
[10] P. Madhusudanan, G. Raju, S. Shankarappa, Hydrogel systems and their role in neural tissue engineering, J. R. Soc. Interface 17 (162) (2020), 20190505.
[11] L. Martinelli, C. Pederzolli, M. Rinaldi, A. Graffigna, N. Pederzolli, M. Vigano, The Use of Fibrin Glue in Thoracic Organ Transplantation: Analysis of 4-Year Experience, Springer Berlin Heidelberg, Berlin, Heidelberg, 1995, pp. 38–42.
[12] M.B. Detweiler, J.G. Detweiler, J. Fenton, Sutureless and reduced suture anastomosis of hollow vessels with fibrin glue: a review, J. Invest. Surg. : the official journal of the Academy of Surgical Research 12 (5) (1999) 245–262.
[13] A.B. Cho, T.H. Wei, L.R. Torres, R.M. Júnior, G.M. Rugiero, M.A. Aita, Fibrin glue application in microvascular anastomosis: comparative study of two free flaps series, Microsurgery 29 (1) (2009) 24–28.
[14] D.H. Sierra, Fibrin sealant adhesive systems: a review of their chemistry, material properties and clinical applications, J. Biomater. Appl. 7 (4) (1993) 309–352.
[15] J. Li, A. Celiz, J. Yang, Q. Yang, I. Wamala, W. Whyte, B. Seo, N. Vasilyev, J. Vlassak, Z. Suo, Tough adhesives for diverse wet surfaces, Science 357 (6349) (2017) 378–381.
[16] G.M. Taboada, K.S. Yang, M.J.N. Pereira, S.H.S. Liu, Y.S. Hu, J.M. Karp, N. Artzi, Y. H. Lee, Overcoming the translational barriers of tissue adhesives, Nature Reviews Materials 5 (4) (2020) 310–329.
[17] J.E. Murray, The first successful organ transplants in man, J. Am. Coll. Surg. 200 (1) (2005) 5–9.
[18] D. Hamilton, A History of Organ Transplantation: Ancient Legends to Modern Practice, University of Pittsburgh Pre, 2012.
[19] C.J.E. Watson, J.H. Dark, Organ transplantation: historical perspective and current practice, Br. J. Anaesth. 108 (2012) I29–I42.
[20] A. Carrel, La technique opératoire des anastomses vasculaires et la transplantation des viscères, Lyon Med. 98 (1902) 859–864.
[21] Alexis Carrel – Nobel Lecture. NobelPrize.org. Nobel Prize Outreach AB 2021. Mon. 8 Nov 2021. <https://www.nobelprize.org/prizes/medicine/1912/carrel/lecture/ .
[22] X.-G. Zhang, X.-M. Liu, S.-P. Wang, Q. Lu, A.-H. Shi, Y. Li, Y.-R. Qian, K. Liu, F. Ma, H.-H. Wang, Y.-L. Li, R. Wu, X.-F. Zhang, B. Wang, Y. Lv, Fast vascular reconstruction with magnetic devices in liver transplant: a novel surgical technique, Liver Transplant. 27 (2) (2020) 286–290.
[23] A.J. IJtsma, C.S. van der Hilst, M.T. de Boer, K.P. de Jong, P.M. Peeters, R.J. Porte, M.J. Slooff, The clinical relevance of the anhepatic phase during liver transplantation, Liver Transplant. 15 (9) (2009) 1050–1055.
[24] J.-Y. Sun, X. Zhao, W.R. Illeperuma, O. Chaudhuri, K.H. Oh, D.J. Mooney, J. J. Vlassak, Z. Suo, Highly stretchable and tough hydrogels, Nature 489 (7414) (2012) 133–136.
[25] H. Yuk, T. Zhang, S. Lin, G.A. Parada, X. Zhao, Tough bonding of hydrogels to diverse non-porous surfaces, Nat. Mater. 15 (2) (2016) 190–196.
[26] J. Liu, Y. Pang, S. Zhang, C. Cleveland, X. Yin, L. Booth, J. Lin, Y.-A.L. Lee, H. Mazdiyasni, S. Saxton, Triggerable tough hydrogels for gastric resident dosage forms, Nat. Commun. 8 (1) (2017) 1–10.
[27] G. Deng, F. Li, H. Yu, F. Liu, C. Liu, W. Sun, H. Jiang, Y. Chen, Dynamic hydrogels with an environmental adaptive self-healing ability and dual responsive sol-gel transitions, ACS Macro Lett. 1 (2) (2012) 275–279.
[28] C. Ni, D. Chen, Y. Zhang, T. Xie, Q. Zhao, Autonomous shapeshifting hydrogels via temporal programming of photoswitchable dynamic network, Chem. Mater. 33 (6) (2021) 2046–2053.
[29] L. Imbernon, E.K. Oikonomou, S. Norvez, L. Leibler, Chemically crosslinked yet reprocessable epoxidized natural rubber via thermo-activated disulfide rearrangements, Polym. Chem. 6 (23) (2015) 4271–4278.
[30] L. Zhang, W. Liu, L. Lin, D. Chen, M.H. Stenzel, Degradable disulfide core-cross-linked micelles as a drug delivery system prepared from vinyl functionalized nucleosides via the RAFT process, Biomacromolecules 9 (11) (2008) 3321–3331.
[31] M.C. Darnell, J.-Y. Sun, M. Mehta, C. Johnson, P.R. Arany, Z. Suo, D.J. Mooney, Performance and biocompatibility of extremely tough alginate/polyacrylamide hydrogels, Biomaterials 34 (33) (2013) 8042–8048.
[32] H. Yang, C. Li, J. Tang, Z. Suo, Strong and degradable adhesion of hydrogels, ACS Applied Bio Materials 2 (5) (2019) 1781–1786.
[33] P.A. Leggat, D.R. Smith, U. Kedjarune, Surgical applications of cyanoacrylate adhesives: a review of toxicity, ANZ J. Surg. 77 (4) (2007) 209–213.
[34] B. Chen, J. Yang, R. Bai, Z. Suo, Molecular staples for tough and stretchable adhesion in integrated soft materials, Advanced Healthcare Materials 8 (19) (2019) 1900810.
[35] J. Ennker, I.C. Ennker, D. Schoon, H.A. Schoon, S. Dörge, M. Meissler, M. Rimpler, R. Hetzer, The impact of gelatin-resorcinol glue on aortic tissue: a histomorphologic evaluation, J. Vasc. Surg. 20 (1) (1994) 34–43.
[36] D.G. Wallace, G.M. Cruise, W.M. Rhee, J.A. Schroeder, J.J. Prior, J. Ju, M. Maroney, J. Duronio, M.H. Ngo, T. Estridge, G.C. Coker, A tissue sealant based on reactive multifunctional polyethylene glycol, J. Biomed. Mater. Res. 58 (5) (2001) 545–555.
[37] X. Zhao, X. Chen, H. Yuk, S. Lin, X. Liu, G. Parada, Soft materials by design: unconventional polymer networks give extreme properties, Chem. Rev. 121 (8) (2021) 4309–4372.
[38] J. Yang, R. Bai, B. Chen, Z. Suo, Hydrogel adhesion: a supramolecular synergy of chemistry, topology, and mechanics, Adv. Funct. Mater. 30 (2) (2020) 1901693.
[39] C. Reddy, D. Pennington, H. Stern, Microvascular anastomosis using the vascular closure device in free flap reconstructive surgery: a 13-year experience, J. Plast. Reconstr. Aesthetic Surg. : JPRAS 65 (2) (2012) 195–200.
[40] F.M. Leclère, V. Duquennoy-Martinot, M. Schoofs, B. Buys, S. Mordon, [Thirty years of laser-assisted microvascular anastomosis (LAMA): what are the clinical perspectives?], Neurochirurgie 57 (1) (2011) 1–8.
[41] K. Tachi, K.S. Furukawa, I. Koshima, T. Ushida, New microvascular anastomotic ring-coupling device using negative pressure, J. Plast. Reconstr. Aesthetic Surg. : JPRAS 64 (9) (2011) 1187–1193.